IMPROVEMENT IN THE DETECTION OF LAND COVER CLASSES USING THE WORLDVIEW-2 IMAGERY

Ahmed Elsharkawy [1,2], Mohamed Elhabiby [1,3] & Naser El-Sheimy [1,4]
[1]Dept. of Geomatics Engineering, University of Calgary
Calgary, Alberta, T2N 1N4
Phone: 403-210-7897, Fax: 403-284-1980,
[2]Email: askelsha@ucalgary.ca
[3]Public Works Department, Faculty of Engineering, Ain Shams University, Cairo, Egypt.
Email: mmelhabi@ucalgary.ca
[4] Email: elsheimy@ucalgary.ca

ABSTRACT

Recent advances in satellite and airborne sensors make spatial and multispectral high-resolution imagery effortlessly available. These advances give the chance to address and solve some old problems related to the poor spatial or spectral resolution; such as the lack of details for certain features or the inability of the traditional classifiers to detect some land cover types due to the missing of important parts of the spectrum. High-resolution imagery is particularly well suited to urban applications. Previous High-resolution imagery data sources (such as IKONOS or QuickBird) did show the required spatial details necessary to provide a good urban planning solution, but they fail to represent a reasonable spectral resolution, as they only contain three visible bands and one near infra red band, which hinders the ability of traditional spectral classifiers to accurately detect some land-cover types . The increased spatial information in sub-meter imagery accompanied with a low spectral resolution make the process of image classification using traditional supervised or unsupervised spectral classification algorithms a very difficult task. The previous limitations led many researchers to the object-oriented solution to provide a reliable classification results. This study evaluated how spectral and spatial resolution of the new satellite World View-2 influences the quality of the classification using only traditional spectral classifiers which mainly depends on the information provided by the 8-spectral bands ranging from the visible to mid-infra red bands, investigating the rule of the new bands in accurately distinguishing detailed land cover types.

This study assesses the accuracy of the classification for a data set of WorldView-2 satellite imagery when using the full 8-bands (data set I), and when using only the three-visible bands and the NIR band only (data set II). The study uses the Maximum Likelihood Classifier method for extracting land cover information. Also the study introduces new band ratios in a multi-layer classification tree analysis to extract certain features such as shadows and asphalt roads.

KEYWORDS: high resolution satellite imagery, supervised classification, land cover, pixel based, new bands.

INTRODUCTION

Recent advances in satellite imagery resulted in the availability of high-resolution multispectral and spatially accurate imagery. High-resolution satellite imagery is exceptionally well fitted to urban applications such as change detection[1]. Medium resolution satellites such as Landsat TM did not provide the required spatial detail necessary for many urban planning applications. In the past, automated image classification techniques entirely relied on the pixel characteristics such as its digital number or colour, leaving behind the important characteristics of texture, shape and context[2]. The previous limitation could be acceptable in low or medium resolution satellite imagery as the pixel is relatively large and already contains texture information. However, in case of high resolution satellite imagery the pixel is relatively small and the texture information occurs in the relationship between pixels is quite meaningful.

In addition to the large-scale collection capacity of WorldView-2's it has a high spatial and spectral resolution. According to [3] this satellite is able to capture 46 cm panchromatic imagery and 1.84 m spectral resolution with 8-band multispectral imagery. The high spatial resolution facilitate the differentiation of fine details, like vehicles, shallow reefs and individual trees, while the high spectral resolution provides detailed information on such diverse areas as the quality of the road surfaces, the depth of the ocean, and the health of plants[3].

WorldView-2 is the first commercial high-resolution satellite to provide 8 spectral sensors in the visible to near-infrared range. Each sensor is closely focused on a particular range of the electromagnetic spectrum, which is sensitive to a specific feature on the ground. In concert, they are designed to improve the segmentation and classification of land and marine features[3]. Figure 1. Panchromatic and multispectral wavelengths for different satellites, is a quick comparison between QuickBird, WorldView-1 and WorldView-2 regarding their spectral and panchromatic bands.

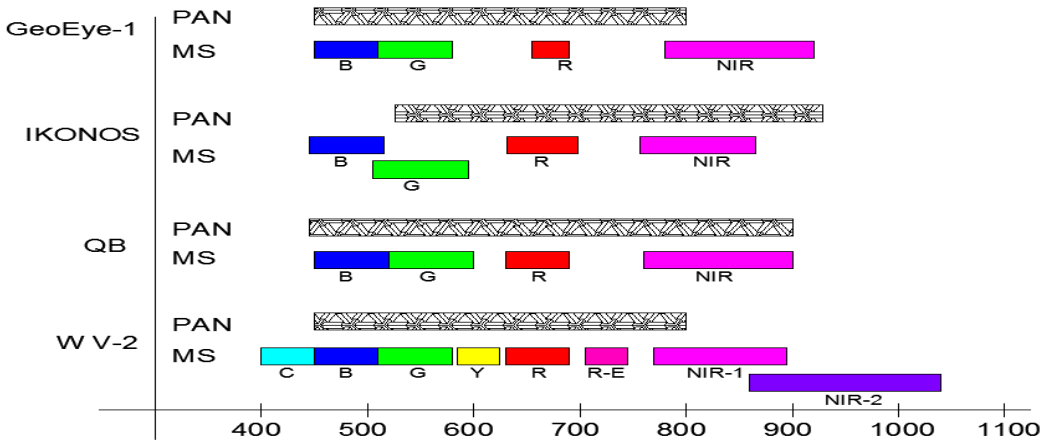

Figure 1. Panchromatic and multispectral wavelengths for different satellites,[4]

Generally, The new spectral bands in WorldView-2, Coastal blue, Yellow, Red edge and NIR-2, is targeting costal and vegetation land cover types with applications in plant species identification, mapping of vegetation stress and crop types, wetlands, coast water quality, and bathymetry [5] . To be more specific, the Yellow and Red edge bands are filling important gaps in the spectrum that relate to the ability of capturing vegetation [6]. Moreover, Coastal blue and NIR2 bands is very helpful to discriminate among different types of vegetation and many man-made objects [7]. This study applies a robust framework to WorldView-2 images to validate the efficiency and the predictive role of the four new spectral bands for improved land cover classification based on the pixel information only compared to object oriented approach using classification tree analysis.

DATA AND METHOD

Area of Study

The study area is a residential area in Ismailia city about 120 Km to the north east direction from Cairo the capital of EGYPT. The study area is an urban area comprises scattered buildings, roads, vegetation areas, shadowed areas, shoreline and water body. The data was provided by Digital Globe, http://www.digitalglobe.com, the images was captured on April 7th, 2011 in morning time. Figure 3 illustrates part of the study area, 598X793, false color composite, NIR-1 G B.

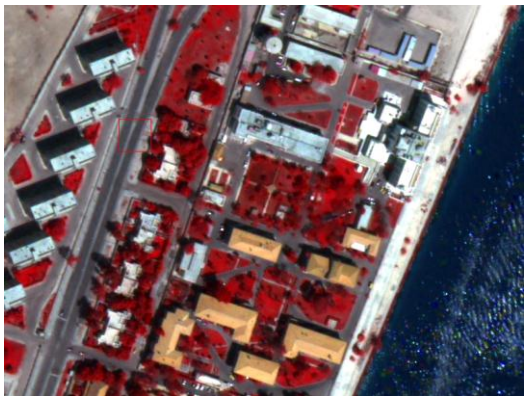

Figure 3. Area of study.

Methodology

For the purpose of the study, two data sets will be generated from this data, as there is no IKONOS or QUICKBIRD data were available, one will be notified by (Data Set I), in which it comprises the full 8-bands, and the other will be notified by (Data Set II), in which the four new bands will be omitted and it will contain only the 3-visible bands and the NIR-1, as in the next figure.

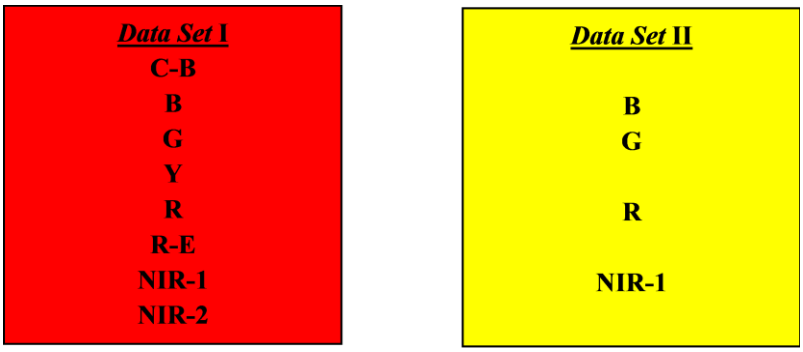

Figure 4. Data set used.

Generally, any imagery will be used in radiometric/spectral analysis must be converted to spectral radiance at a minimum or top of atmosphere reflectance in order to account for the variation in the relative positions between the sun, the earth and the satellite to obtain an absolute values for the NDVI ratios can be applied in any other scene [8]. Converting the Digital Numbers (DN) to Top of Atmosphere (ToA) reflectance is a two-step process. First DNs are converted to ToA radiance values. Then these radiance values are then converted to reflectance values[9].

Conversion to Top-of-Atmosphere Spectral Radiance. According to [10] WorldView-2 products are delivered to the customer as radiometrically corrected image pixels. The values of these pixels are calculated as a function of the amount of the spectral radiance enters the telescope aperture and the instrument conversion of that radiation into a digital signal. Therefore, image pixel data are unique to WorldView-2 and should not be directly compared to imagery from other sensors in a radiometric/spectral sense. Instead, image pixels should be converted to top-of-atmosphere spectral radiance at a minimum. Top-of-atmosphere spectral radiance is defined as the spectral radiance entering the telescope aperture at the WorldView-2 altitude of 770 km. The conversion from radiometrically corrected image pixels to spectral radiance uses the following general equation for each band of a WorldView-2 product[8]:

$$L_{\lambda_{pixel,band}} = \frac{K_{band} \cdot q_{pixel,band}}{\Delta\lambda_{band}} \qquad \text{Eq. 1}$$

where, $L_{\lambda_{pixel,band}}$ are the top-of-atmosphere spectral radiance image pixels [$W.m^{-2}.sr^{-1}.\mu m^{-1}$],

K_{band} is the absolute radiometric calibration factor [$W.m^{-2}.sr^{-1}.count^{-1}$] for a given band,

$q_{pixel,band}$ are the given radiometrically corrected image pixels [counts] and

$\Delta\lambda_{band}$ is the effective bandwidth [μm] for a given band

Both K_{band} and $\Delta\lambda_{band}$ can be found in the image metadata files (*.IDM) attached with the WorldView-2 product under the names (absCalFactor) and (effectiveBandwidth) respectively. The following table summarize both of these quantities for both the panchromatic and the 8 multi-spectral bands.

Table 1. Absolute radiometric calibration and effective bandwidth for the given bands

Band name	K_{band} W.m^{-2}.sr^{-1}.count^{-1}	$\Delta\lambda_{band}$ μm
PAN	5.68E-02	2.85E-01
C	9.30E-03	4.73E-02
B	1.78E-02	5.43E-02
G	1.36E-02	6.30E-02
Y	6.81E-03	3.74E-02
R	1.10E-02	5.74E-02
R-E	6.06E-03	3.93E-02
NIR1	1.22E-02	9.89E-02
NIR2	9.04E-03	9.96E-02

Conversion to Top-of-Atmosphere Spectral reflectance. Right now we have the ToA spectral radiance. However, this top-of-atmosphere spectral radiance varies with Earth-Sun distance, solar zenith angle, topography, bi-directional reflectance distribution function (BRDF-the target reflectance varies depending on the illumination and observation geometry), and atmospheric effects (absorption and scattering)[8]. As mentioned earlier that converting multispectral data into reflectance before performing spectral analysis techniques such as band ratios, Normalized Difference Vegetation Index (NDVI), matrix transformations, etc., is a must. For each scene the distance between the sun and earth in astronomical units, the day of the year (Julian date), and solar zenith angle must be known.

$$JD = int[356.25.(year + 4716)] + int[30.6001.(month + 1)] + day + \frac{UT}{24} + B - 1524.5 \qquad \text{Eq. 2}$$

$$d_{ES}=1.00014-0.01671.\cos(g)-0.00014.\cos(2g) \qquad \text{Eq. 3}$$

The Earth-Sun distance will be in Astronomical Units (AU) and should have a value between 0.983 and 1.017. For the WorldView-2 launch date, October 8, 2009 at 18:51:00 GMT corresponds to the Julian Day 2455113.285; the Earth-Sun distance is 0.998987 AU. At least six decimal places should be carried in the Earth-Sun distance for use in radiometric balancing or top-of atmosphere reflectance calculations[8].
The average solar Zenith angle has to be calculated for the whole scene at the time of acquisition according to the following equation

$$\theta_s = 90.0 - sunEL \qquad \text{Eq. 4}$$

where *sunEl* value can be found in the same file *.IDM

Now we can convert the radiance values to ToA reflectance values using the following equation

$$\rho_{\lambda_{pixel,band}} = \frac{L_{\lambda_{pixel,band}}.{d_{ES}}^2.\pi}{E_{sun\lambda_{band}}.\cos(\theta_s)} \qquad \text{Eq. 5}$$

where $\rho_{\lambda_{pixel,band}}$ are the ToA reflectance values
$L_{\lambda_{pixel,band}}$ are the ToA radiance values
d_{ES} is the Earth-Sun distance in Astronomical Units (AU)
$E_{sun\lambda_{band}}$ WorldView-2 Band-Averaged Solar Spectral Irradiance [8]
θ_s The average solar Zenith angle

To get the most gain of the spatial resolution capability of the Worldview-2 data a fusion technique has to be applied. The proposed algorithm begins with a data fusion between the panchromatic band of the Worldview-2 data, 0.50 m, and the multispectral ones, 2.00 m resolution, to generate 8-spectral bands with a resolution of 0.50 m. One

of the most common fusion techniques is the Brovey Transform. This technique is optimum when increase in contrast in the low and high ends of an images histogram (i.e., to provide contrast in shadows, water, and high reflectance areas such as urban features) is needed. The procedure of this transform starts with multiplying each Multi-Spectral, MS, band by the high-resolution Panchromatic, PAN, band, and then divides each product by the sum of the MS bands. Since the Brovey Transform is intended to produce RGB images, only three bands at a time should be merged from the input multispectral scene[11] in our case we choose NIR-1, Green and Blue bands.

The study uses two different methods for extracting land cover information;

1) Supervised classification approach using the Maximum Likelihood Classifier,

2) Image classification using multi-layer classification tree analysis. In the following sections the details of these methods will be demonstrated.

Supervised Classification Approach using the Maximum Likelihood Classifier

For the purpose of applying Maximum Likelihood Classifier training pixels for six classes; asphalt roads, vegetation, Bright surface, red roofs, shadow, water and bare soil, were chosen for the two data sets (I,II). Table 2 summarizes the number of pixels used for training and verification for each class.

Table 2. Training and verification pixels summary

Class name	Training pixels No.	Validation pixels No.	Total
Asphalt roads	3798	3484	7282
Vegetation	6984	2936	9920
Bright surface	4280	4726	9006
Red roofs,	2710	1551	4261
Shadow	1278	934	2212
Water	23467	3823	27290
Bare soil	5872	783	6655
Total	48389	18237	66626

The classification results were compared with the validation pixels, as ground truth data, to assess the overall accuracy. The error matrix was generated to obtain the user's and producer's accuracy [12]. The user's accuracy refers to the measure of commission errors that correspond to those pixels from other classes that the classifier has labeled as belonging to the class of interest. Moreover, the producer's accuracy refers to the measure of omission errors that correspond to those pixels belonging to a class of interest that the classifier didn't recognize [13, 14].

Evaluation of Training Sets. In order to evaluate certain training data sets against specific classes it is common to run statistical measures of distances between two signatures for all possible combination of bands that is used in the classification. This process will help us to rule out any bands that are not useful in the results of the classification. In remote sensing literature, the most popular separability measures are the separability indices; namely, divergence, transformed divergence, Bhattacharyya distance and Jeffries-Matusita distance[15].

For instance, one of the most popular separability measures, divergence, is computed using the mean and variance-covariance matrices of the data representing feature classes. While, the transformed divergence measure, the one we used in this research paper, can be considered as the standardized form of divergence as it scales the divergence values to a certain range, 0 to 2 here. Generally, pairs with values greater than 1.9 indicate that the ROI pairs have good separability. Separability of the training pixels for all possible combinations was calculated for the 2 data sets and the results were as in the figure 5.

The formula for computing the divergence (D_{ij}) is as follows:

$$D_{ij} = \frac{1}{2} tr\left(\left(C_i - C_j\right)\left(C_i^{-1} - C_j^{-1}\right)\right) + \frac{1}{2} tr\left(\left(C_i^{-1} - C_j^{-1}\right)\left(\mu_i - \mu_j\right)\left(\mu_i - \mu_j\right)^T\right) \quad \text{Eq. 6}$$

where:

i and *j* = the two signatures (classes) being compared

C_i = the covariance matrix of signature *i*

μ_i = the mean vector of signature *i*

tr = the trace function (matrix algebra)

T = the transposition function

And the formula for computing the transformed divergence (TD_{ij}) is as follows:

$$TD_{ij} = 2000(1 - \exp(\frac{-D_{ij}}{8})) \quad \text{Eq. 7}$$

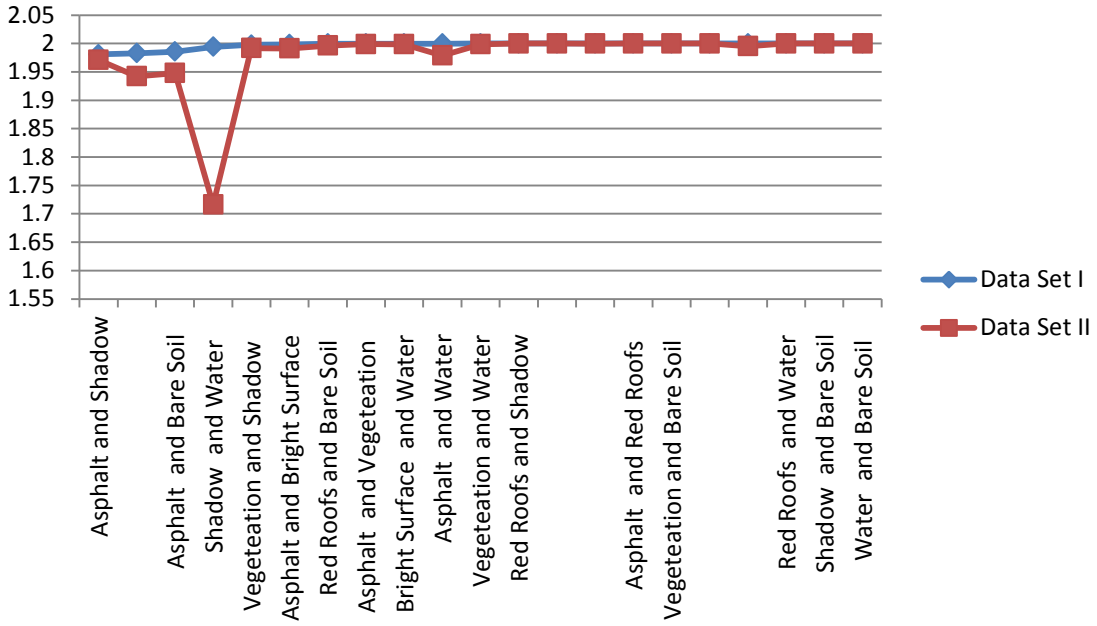

Figure 5. Separability values for all possible pairs for the 2 data sets.

Supervised Classification Approach using the New Band Ratios

The traditional NDVI ratio plus two new band ratios are introduced, the original NDVI (R1) specially suited for vegetation and water, second one (R2) to detect asphalt, shadow and man-made objects and finally (R3) to detect red roofs, buildings and barren. Table 5 summarizes the three ratios and their usage.

Table 3. Band ratios and their implementation

	Band ratio	Target classes	Ratio range
R1	$\frac{R - NIR1}{R + NIR1}$	Vegetation Water	-0.5 – 0.07
R2	$\frac{C - R}{C + R}$	Asphalt Shadow Manmade object	-0.30 – 0.2
R3	$\frac{NIR1 - Y}{NIR1 + Y}$	Red roof Building Barren	-0.075 – 0.50

R1 is applied first to separate the image into vegetation and non vegetation, and then R2 is applied to detect the water above certain threshold and Asphalt, shadow and red roofs are detected within lower and upper thresholds, finally the R3 ratio is applied to detect Bright surfaces below certain threshold. Figure 6 summarize theses steps along with the applied thresholds.

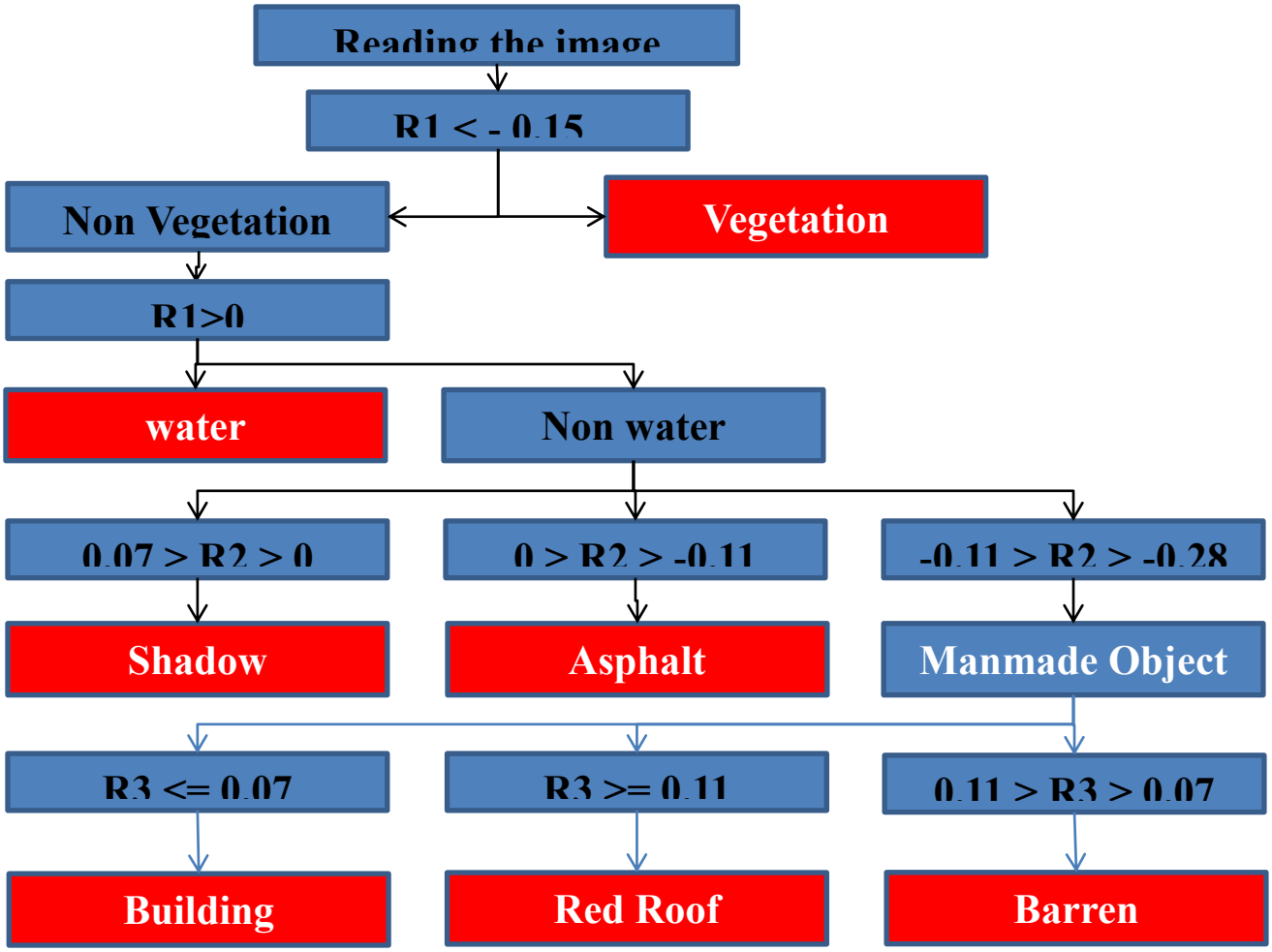

Figure 6. Applying the band ratios with the proposed thresholds.

RESULTS AND ANALYSIS

Supervised Classification Eesults using MLC

Classification results for the data set I. Table 4 summarizes the confusion matrix of the data set I against the verification pixels, table 2, the overall Accuracy was 99.3% and the Kappa Coefficient was 0.9907.

Table 4. Confusion matrix for the data set I

	Asphalt	Vegetation	Bright Surface	Red Roofs	Shadow	Water	Bare Soil	Total
Asphalt	99.54	0.00	0.11	0.00	1.21	0.00	2.30	10.93
Vegetation	0.14	99.95	0.00	0.00	0.82	0.00	0.00	14.89
Bright Surface	0.25	0.04	99.13	0.00	0.43	0.01	1.38	13.52
Red Roofs	0.04	0.01	0.00	100.00	0.09	0.00	0.00	6.40
Shadow	0.00	0.00	0.00	0.00	95.75	0.01	0.00	3.32
Water	0.00	0.00	0.71	0.00	1.69	99.98	0.00	40.96
Bare Soil	0.03	0.00	0.04	0.00	0.00	0.00	96.32	9.99
Total	100.00	100.00	100.00	100.00	100.00	100.00	100.00	100.00

Classification results for the data set II. Table 5 summarizes the confusion matrix of the data set II against the verification pixels, table 2, the overall Accuracy was 97.5280% and the Kappa Coefficient was 0.9679.

Table 5. Confusion matrix for the data set II

	Asphalt	Vegetation	Bright Surface	Red Roofs	Shadow	Water	Bare Soil	Total
Asphalt	99.51	0.00	0.09	0.00	0.87	0.30	2.25	11.03
Vegetation	0.14	99.98	0.00	0.00	1.26	0.03	0.00	14.92
Bright Surface	0.25	0.01	98.62	0.35	0.13	0.15	2.04	13.58
Red Roofs	0.07	0.01	0.00	99.65	0.00	0.00	0.01	6.37
Shadow	0.00	0.00	0.00	0.00	93.37	3.28	0.00	4.57
Water	0.00	0.00	0.57	0.00	4.38	96.25	0.00	39.51
Bare Soil	0.03	0.00	0.73	0.00	0.00	0.00	95.70	10.02
Total	100.00	100.00	100.00	100.00	100.00	100.00	100.00	100.00

Figures 7, 8 and 9 illustrate the classification results for the data sets and the user's and producer's accuracy comparisons respectively.

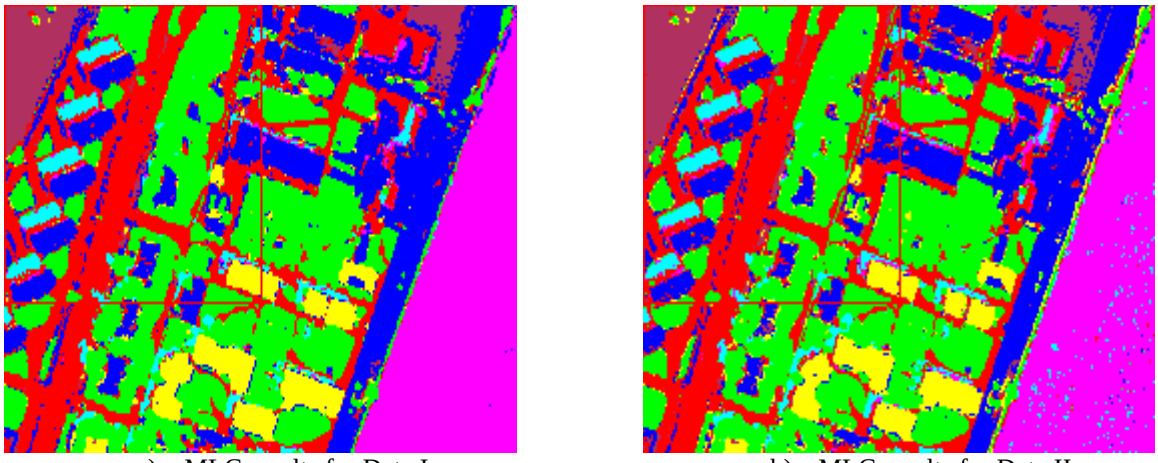

a) MLC results for Data I b) MLC results for Data II

Figure 7. Supervised classification results for the two data set.

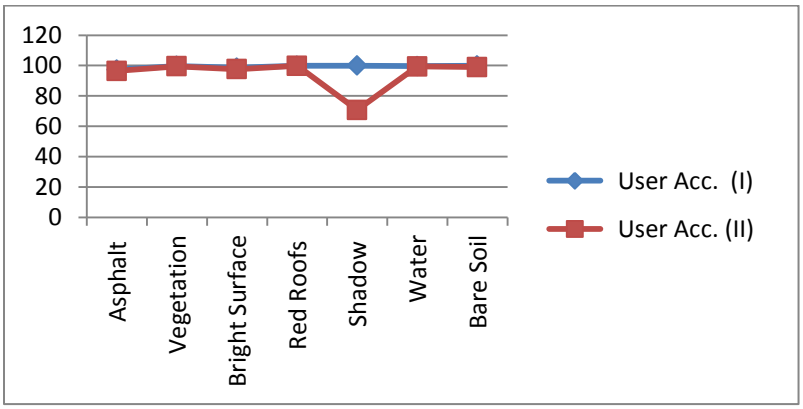

Figure 8. User's accuracy comparison for the two data set.

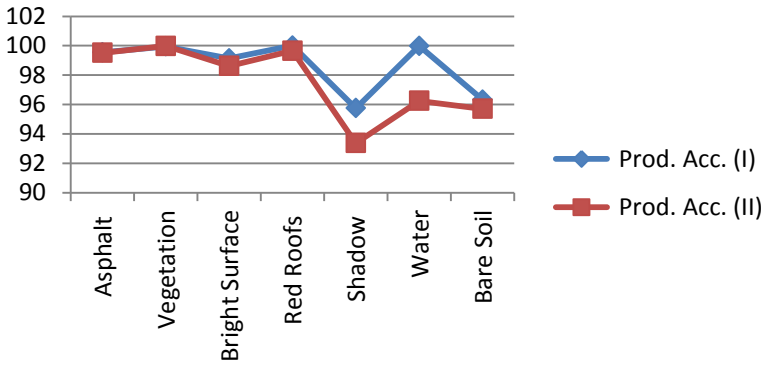

Figure 9. Producer's accuracy comparison for the two data set.

Supervised Classification Results using Band Ratios

Applying the band ratios in the shown sequence as in figure 6 showed good results. Water, vegetation, manmade objects and shadow were all successfully classified using the 3 band ratios without any spatial attributes, in which it will give a good solution for those who need fast and reliable land cover types. The original image and the classified image are shown in figures 10 and 11 respectively.

Figure 10. Area of study.

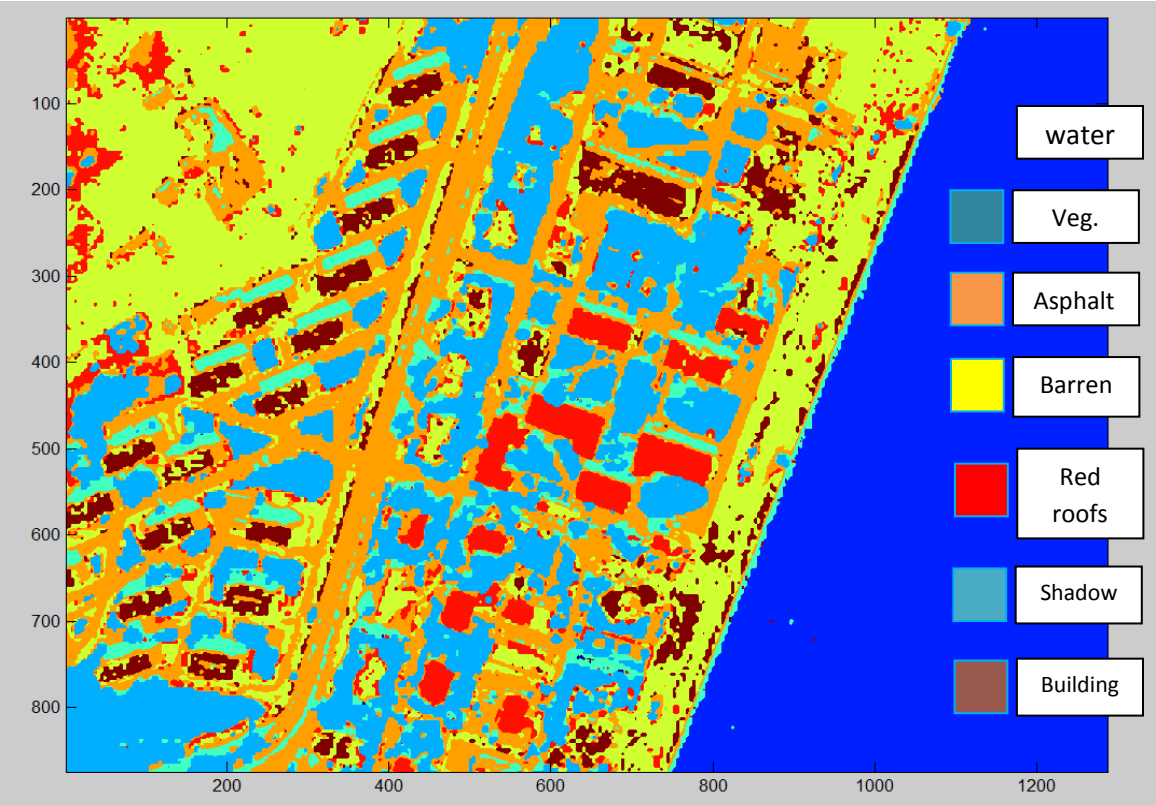

Figure 11. Classification results for the proposed band ratios.

Analysis of the results

For the first approach, MLC, visual inspection showed better results for the data set I than the data set II. Statistically, both the overall accuracy and kappa coefficients were enhanced by 3% higher, than those of data set II. Consequently, user's and producer's accuracy were higher for data set I relative to data set II for all classes as shown in figure 8, 9. Even for the separability analysis the 8-band combination gives better separability measures for all class combinations comparing to the 4-band combination as in figure 5.

Regarding the multi-layer classification approach, applying the band ratios in the shown sequence in figure 6, results in good delineation of vegetation, asphalt, shadow, water, red roofs and bright surfaces. The new bands namely C, Y, Red edge and NIR2 showed very good potentials for detecting manmade objects and vegetation as well.

CONCLUSION

High spectral and spatial resolution of some data such as WorldView-2 may offer challenges in mapping urban features. Water, Shadow, Red roofs and bright surfaces classes spectrally exhibit a great deal of confusion either due to the high similarity in spectral response, as in the first two classes, or due to the similarity in material type, as in the later two classes.

In this research paper a full study to the new satellite mission Worldview-2 has been done with focus on the potentials of the new spectral bands for efficient classification. Two data sets were generated from the same available data by eliminating the four new bands in one set and using the full eight bands in the other. The study was executed using two supervised classification approaches; one with the well known MLC for two data sets generated from the same data by eliminating the new bands from one set and using the full 8-bands in the other and comparing the classification results of both. The second approach used the new bands in a multi-layer classification process to detect different land cover type's ranges from water to vegetation and finally manmade objects. Both approaches used only the spectral attributes of the given data.

All classification results were in favor of the full eight bands set for all the studied classes, also the separability statistics was better in case of the full eight band set. In general, the new bands showed promising results towards manmade objects, water, shadow and vegetation.

REFERENCES

[1] N. Thomas, *et al.*, "A comparison of urban mapping methods using high-resolution digital imagery," *Photogrammetric Engineering and Remote Sensing*, vol. 69, pp. 963-972, Sep 2003.

[2] K. M. S. Sharma and A. Sarkar, "Modified contextual classification technique for remote sensing data," *Photogrammetric Engineering and Remote Sensing*, vol. 64, pp. 273-280, Apr 1998.

[3] D. Globe. (2009, the Benefits of the 8 Spectral Bands of WorldView-2. *White Paper*, 12.

[4] A. Elsharkawy, *et al.*, "A modified parallelepiped-like method for supervised classification for high resolution satellite imagery " presented at the CGU Annual Scientific Meeting, Banff, Calgary, 2011.

[5] G. Marchisio, *et al.*, "On the relative predictive value of the new spectral bands in the WorldWiew-2 sensor," in *Geoscience and Remote Sensing Symposium (IGARSS), 2010 IEEE International*, 2010, pp. 2723-2726.

[6] H. Shafri, *et al.*, "Hyperspectral Remote Sensing of Vegetation Using Red Edge Position Techniques," *American Journal of Applied Sciences*, vol. 3(6), pp. 1864-1871, 2006.

[7] M. Herold, *et al.*, "THE SPECTRAL DIMENSION IN URBAN LAND COVER MAPPING FROM HIGHRESOLUTION OPTICAL REMOTE SENSING DATA," *The 3rd Symposium on Remote Sensing of Urban Areas*, p. 8, june 2002 2002.

[8] T. Updike and C. Comp, "Radiometric Use of WorldView-2 Imagery," D. Globe, Ed., ed, 2010.

[9] T. Y. C. f. E. Observation. (2010). *Converting Digital Numbers to Top of Atmosphere (ToA) Reflectance*. Available: http://www.yale.edu/ceo

[10] D. Globe, "DigitalGlobe Core Imagery Products Guide," D. Globe, Ed., ed, 2009.

[11] K. G. Nikolakopoulos, "Comparison of nine fusion techniques for very high resolution data," *Photogrammetric Engineering and Remote Sensing*, vol. 74, pp. 647-659, May 2008.

[12] R. G. Congalton, "A REVIEW OF ASSESSING THE ACCURACY OF CLASSIFICATIONS OF REMOTELY SENSED DATA," *Remote Sensing of Environment*, vol. 37, pp. 35-46, Jul 1991.

[13] J. A. Richards and X. Jia. (2006). *Remote Sensing Digital Image Analysis (4th ed.)*.

[14] S. Bhaskaran, *et al.*, "Per-pixel and object-oriented classification methods for mapping urban features using Ikonos satellite data," *Applied Geography*, vol. 30, pp. 650-665, Dec 2010.

[15] T. Kavzoglu and P. M. Mather, "The Use of Feature Selection Techniques in the Context of Artificial Neural Networks," in *26th Annual Conference of the Remote Sensing Society*, Leicester, UK, 2000.